

An experimental testing system for fibre-reinforced-polymer-strengthened concrete panels under uniform pressure loads

J Helm^{1*}, S Kurtz², A-R Salkini², and E O'Brien¹

¹Department of Mechanical Engineering, Lafayette College, Easton, Pennsylvania, USA

²Department of Civil and Environmental Engineering, Lafayette College, Easton, Pennsylvania, USA

The manuscript was received on 24 February 2008 and was accepted after revision for publication on 22 April 2008.

DOI: 10.1243/03093247JSA422

Abstract: A testing system to investigate the response of large (2 m×2 m) concrete panels strengthened with fibre-reinforced polymer (FRP) to uniform pressure loads has been developed. The system combines a test frame that employs pressurized bladders to produce a uniform load on the lower compressive side of the concrete panels while the upper tensile surface is imaged by two three-dimensional digital image correlation systems. From the images taken of the panel under load, full-field displacement and strain fields are measured. The test programme studies the effects of various types of fibre reinforcement and the effect of fibre orientation on the strength and rigidity of the concrete panels.

This paper presents the development of the testing method, focusing on the creation of the panel loading system and the application of digital image correlation to the study of concrete panels. It presents data from two of the panel tests, contrasting the response of a control panel without bonded FRP and a test panel with six strips of bonded FRP in a unidirectional pattern.

Keywords: digital image correlation, reinforced concrete, stress analysis, fibre-reinforced polymers

1 BACKGROUND

The need to strengthen existing buildings or bridges arises when there is a change of use (e.g. newer heavier traffic on bridges), damage (e.g. bridge impact by a vehicle), or a construction or design flaw (e.g. missing prestressing tendons). Whereas it is common for steel structures to be strengthened by welding supplemental plates, concrete structures are historically more difficult to retrofit. A strengthening method for concrete structures that has been studied extensively is the fibre-reinforced polymer (FRP) plate-bonding technique where sheets of carbon, glass, and aramid fibre composites are bonded to the outsides of the concrete beams or plates, usually with epoxy resin, providing external tension reinforcement to supplement the structure's internal steel reinforcement. The technique has been studied with extensive experimental [1–7]

and analytical research [8–11]. However, a critical need that remains is the ability to predict accurately the common failure mode of plate debonding in which the FRP plate suddenly peels away from the severely damaged concrete (Fig. 1).

An accurate prediction of the plate-debonding mode requires the ability to predict the distribution of bond stresses along the FRP plate. Early closed-form attempts to predict the distribution of bond stresses focused on the effect of the plate end discontinuity, using the assumption of zero bond slip and linear elastic behaviour [8–10]. However, Mukhopadhyaya and Swamy [12] compared these perfect bond analytical models with a wide range of experimental data and concluded that predicted stresses near the plate end are poorly correlated to debonding failures. Experimental measurements by Kurtz *et al.* [13] showed that these solutions substantially underestimate the steady state stresses that occur away from the plate-end influences, particularly at post-yielding loads.

*Corresponding author: Department of Mechanical Engineering, Lafayette College, Easton, PA, USA. email: helmj@lafayette.edu

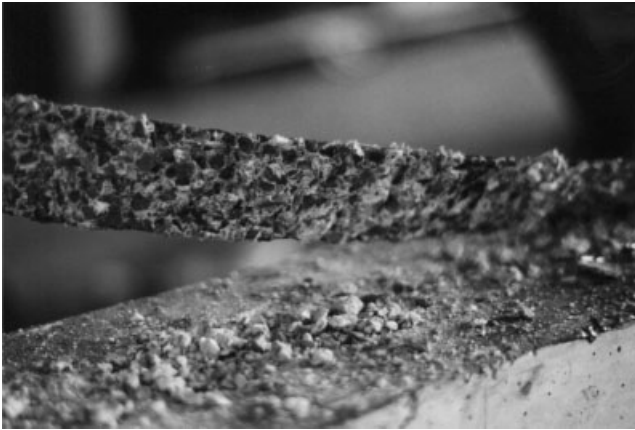


Fig. 1 Typical FRP debonding failure

To overcome the limitations of perfect bond assumptions, Rasheed and Pervaiz [11] developed a simple closed-form solution for the bond stress distribution that considers bond slip. In uniform load tests, Kurtz *et al.* [14] demonstrated that the Rasheed–Pervaiz solution accurately predicts the bond stress distribution while the internal reinforcing steel remains elastic but is a poor predictor once the internal steel yields.

In the uniformly loaded beam tests, Kurtz *et al.* [14] used conventional foil strain gauges at 15 intervals along the length of the FRP to compute the average bond stress in each interval using first differences. This conventional strain gauge approach was also used in the majority of the tests by Kurtz *et al.* [13]. However, duplicate tests were also conducted using digital image correlation (DIC), which confirmed the strain gauge results while overcoming some of the limitations of strain gauge data. Most notably, strain gauges provided information only at discrete points, leaving regions between gauges to be estimated by interpolation, while DIC yields continuous end-to-end strain data.

The present study extends the work of Kurtz *et al.* [13] from one-dimensional beam flexural tests to two-dimensional plate flexural tests. This test programme has important practical use because flat-plate floor systems are the dominant structural type for cast-in-place concrete buildings, outnumbering one-way slab-on-beam floor systems. Yet, the present study shares the same primary objective of earlier beam tests which is to ascertain the distribution of shear stresses between the FRP and the concrete that it is bonded to, as a function of location. While strain gauges remain somewhat practical for beam tests, plate tests prohibit the practical use of strain gauges for two reasons. Firstly, several hundred gauges would be required to obtain

even the crudest information because the plate surface area is 25 times larger than the previous beam surface area. Secondly, because the state of stress is biaxial, strain gauge rosettes would be required, rather than single-axis gauges.

Consequently, DIC was used in this programme because it provides continuous displacement and strain data at substantially better resolution than could be provided by several hundred strain gauge rosettes. To apply this method to the aforementioned problem, a loading system suitable for direct optical observation must be developed and it must be shown that DIC can capture meaningful information about the response of the large-scale plates.

2 TESTING SYSTEM

2.1 Introduction

The testing system for this work was developed to apply an evenly distributed load to the compression side of large plates of concrete while maintaining easily modelled edge conditions and allowing the observation of the specimen's tensile surface by the DIC measurement system. In addition, the system is low cost and easily controllable and works with large-scale (2 m × 2 m) specimens that weigh over 6.6 kN each. Because the load from the system is induced by introducing a volume of water into the load bladders, the tests are run under displacement-type control and are safe to perform even if a panel were suddenly to fail.

2.2 Loading system

To allow the application of the distributed load while maintaining visible access to the tensile surface of the concrete specimen a custom load frame was developed. The frame was designed so that the lower surface of the concrete test panel was subjected to a uniform upward pressure, while the edges were held down with a roller–slider system that allowed out-of-plane edge rotation and horizontal movement perpendicular to the edge direction. Uniform pressure was applied to the test plate using two water-filled bladders. The bladders were inflated using the building water supply and metered by hand with a gate valve. Because of the very large surface area and correspondingly large bladder volume, the rate of pressure increase could be regulated to as slowly as 0.001 kPa/min, although the average rate actually used was about 0.2 kPa/min. The pressure in the bladders was monitored with an electronic pressure

transducer which yielded a resolution of 0.0002 kPa. The bladders were situated in a steel containment basin that provided support when the outer frame was removed to place or remove the concrete specimen and to provide containment if the water bladder should leak or burst.

The outer frame was constructed of 100 mm × 200 mm thick-walled rectangular steel tubing with a stiffened upper plate. Bolted to the outer frame was the sliding rocker assembly, consisting of ultra-high-molecular-weight polyethylene sliders and steel rockers, as shown in Fig. 2. The rocker systems were 127 mm long and centred on each side of the frame. The rockers allowed a range of horizontal movement and out-of-plane rotation at the edge of the specimen. It should be noted that the rockers did not extend all the way along the side of the specimen, allowing unconstrained movement at the corners of the specimen. The forces generated by the pressurized bladders were contained by the strong floor of the structures laboratory, the specimen itself, and the walls of the outer frame. Because no part of the structure crosses over the top of the specimen, and the side wall is close to the same height as the specimen, the loading system does not interfere with visible observation of the tensile surface and is well suited to the image correlation measurements.

2.3 DIC measurement system

The response of the concrete plates to the applied load was measured using two three-dimensional DIC measurement systems. A steel framework was assembled that crossed over the centre of the specimen, approximately 2.5 m above its surface. The framework held the cameras for two separate

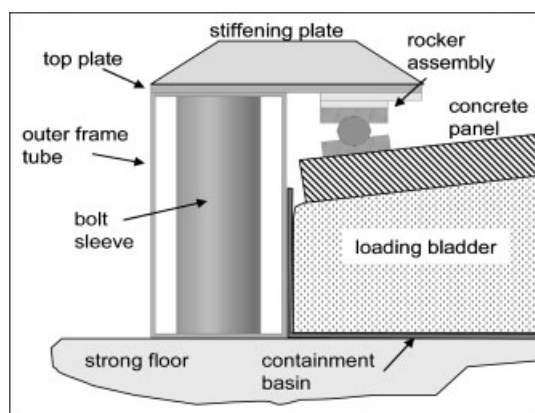


Fig. 2 The test frame: the cross-section showing the frame construction, loading bladder, and specimen

DIC camera systems. Figure 3 shows the locations of the cameras relative to the loading system. The first of the two systems employed 10 mm Schnieder Cinegon lenses to image the entire surface of the specimen. The second DIC system used a pair of 18–35 mm Nikon zoom lenses to image an area one-quarter of the size of the specimen. In both cases the angle between the two cameras was approximately 45°.

A quasi-regular pattern of dots was applied to each area of the specimen to serve as the pattern for the correlation process. The pattern for the global system consisted of dots with an approximate diameter of 7 mm with a 20 mm staggered spacing. The pattern for the local system had 5 mm dots in a 12 mm staggered pattern. The dot pattern was used in the same way as a conventional speckle pattern is used for DIC and, because the dots were not used as discrete markers, variations from dot to dot were acceptable; hence the term quasi-regular is used. For the first two of the 14 tests conducted in the test series the dots were produced using perforated steel as a stencil. For later tests a set of stamps was developed, using a plate of steel with felt dots cemented to the surface, which proved to be both easier to use and significantly faster than the stencil method. Figure 4 shows the dot pattern at the centre of the panel where patterns for both the local and the global camera systems can be seen. The level of uniformity in spacing and size is typical for dots created with the stamping method.

The global and local systems were calibrated using a series of images of a 315 mm × 420 mm calibration target with a 35 mm dot spacing. The target was moved to nine different locations for the large

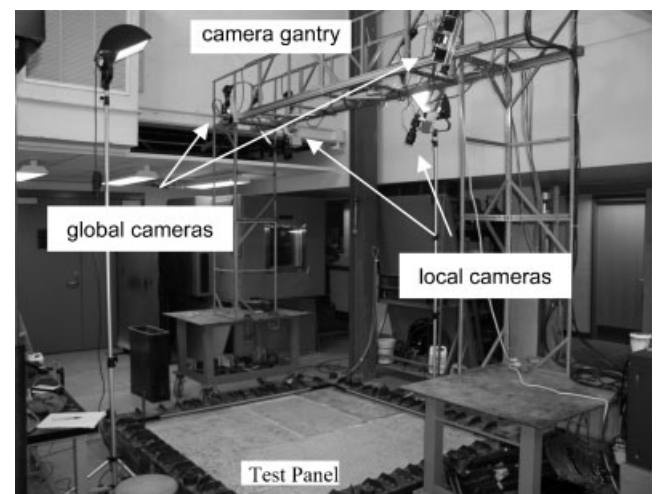


Fig. 3 Test set-up showing the test frame, camera gantry, and global and local camera systems

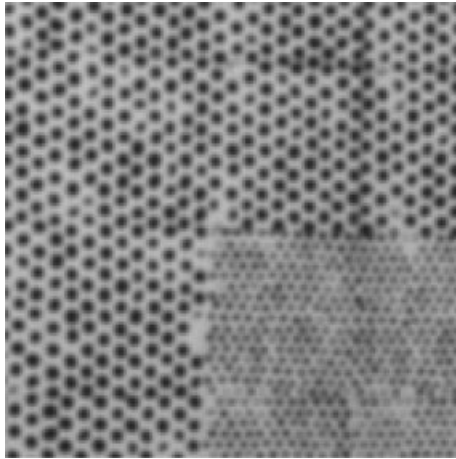


Fig. 4 Stamped quasi-regular patterns in two spatial resolutions for the global and local camera systems

measurement area and five locations in the smaller area. Over 300 image pairs from each DIC system were acquired as the specimen was loaded. The image pairs were then processed to produce approximately 20 000 displacement measurements from each camera system for each load step.

3 EXPERIMENTAL TEST PROGRAMME

3.1 Panel construction, materials, and preparation

Reinforced concrete panels, 2134 mm × 2134 mm × 64 mm, were produced for the test programme. The concrete was made in laboratory batches using 9.5 mm crushed trap coarse aggregate with an average cylinder strength of 30.3 MPa at the time of testing. The panels were reinforced with ASTM A36 bars of 6.35 mm diameter, spaced 150 mm apart, for a reinforcing ratio of about 0.0041. The average yield strength, tensile strength, and elongation of the bars were 314 MPa, 459 MPa, and 27.5 per cent respectively. To improve the steel concrete bond, each bar was coated with a layer of epoxy-bonded coarse sand that was allowed to cure for a week prior to casting.

After casting, the panels were cured for 14 days. Following curing, surface preparation consisted of abrasive grinding with a diamond wheel. For strengthened tests, FRP was then applied to the surface of the specimen. The plates were then painted white and the pattern applied to the surface. The control specimen did not receive any FRP reinforcement, while the reinforced panel had a unidirectional carbon fibre tow sheet with a nominal

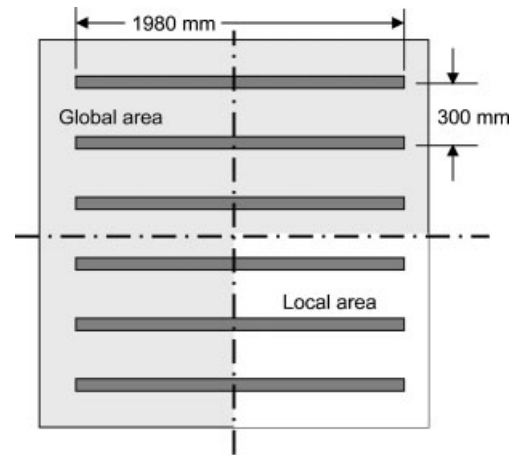


Fig. 5 Strip layout for the FRP-reinforced panel

thickness of 0.165 mm applied to the surface with a two-part saturant epoxy and a two-part primer epoxy. For the strengthened panel reported in this work, six strips of carbon fibre reinforcement were applied. Each strip was 75 mm wide and 1980 mm long and contained two layers of the carbon fibre tow. The strips were all in the nominal X direction of the panel and had a centre-to-centre spacing of 300 mm, as shown in Fig. 5.

3.2 Experimental details

The concrete plates were placed in the loading frame by initially floating the plate on the partially inflated water bladders. At this point in time the bladders were contained and supported by the steel containment basin. The loading frame was then lowered over the specimen and containment basin and bolted to the strong floor. The bladders were then inflated until the specimen was just touching the rocker assemblies. This point was considered the baseline loading point and the initial images were acquired by the DIC systems. The bladders were subsequently inflated to produce pressure changes at a rate of approximately 0.2 kPa/min and images were acquired at 30 s intervals. The load on the specimen was increased until failure.

3.3 Data analysis

Each set of images was analysed with the DIC system to determine the full three-dimensional displacement field for the specimen surface. Because of the large amount of cracking in the specimens, as shown in Fig. 6, a method for automatically rejecting areas where crack growth would interfere with the DIC

process was developed. The quasi-regular pattern of dots used in this work results in correlation values that are more consistent than that achieved with a non-repeating random pattern. The uniformity in correlation values makes it possible to detect cracks by monitoring changes in the correlation value. Unfortunately, the regular pattern also makes it more possible for the correlation method to suffer from false registration. This problem was addressed by limiting the amount the projected subset was allowed to move during the optimization process. The crack exclusion method is explained in detail in reference [15]. The global images were analysed over the three-quarters of the panel covered with the larger dot pattern. Similarly the images from the local system were analysed for the quarter of the panel covered with the smaller pattern. The images were analysed to obtain the initial panel shape, full-field three-dimensional displacements, surface strain components, and principal strains. In addition, the displacements and strains were determined along the centre-line of each FRP strip.

4 RESULTS

This section presents a comparison of the results from an unstrengthened control concrete panel and a panel with six strips of carbon-fibre-reinforced polymer two layers thick. The applied pressure versus centre-point displacement plot, given in Fig. 7, shows that the initial behaviours of the panels are nearly identical for both the control and the FRP panel up to approximately

15 kPa. At this point the behaviours of the two panels diverged. Failure in the panel was assumed when the panel experienced the first significant reduction in pressure despite the addition of more water. The plot shows that the ultimate strength of the panel did not change to any significant degree. The control panel failed at 32.5 kPa and the FRP panel failed at 33.0 kPa. However, the effect of the FRP stiffening is apparent in both the magnitude of the out-of-plane displacements and the nature of the displacements. This stiffening arose because the FRP strips constrain the opening of the cracks in the direction perpendicular to the strips. Failure in the strengthened panel occurred because the crack runs parallel to the FRP strips at $Y = -600$ mm, as seen in Figs 8 and 9.

The out-of-plane displacement fields for the two panels at their respective maximum loads are shown in Fig. 8. Gaps in the presented data result from one of two causes. Firstly, there is a gap that separates the local and global data fields at $X = 0$ mm and $Y = 0$ mm. Secondly, the crack exclusion addition to the DIC program will reject subsets that are significantly affected by the presence of a growing crack. These areas will be seen as gaps in displacement graphs and as areas without shading or contours in contour plots. As seen in the figure, the FRP panel deformed to about half of the maximum displacement of the control panel. In addition, the effect on the deformation behaviour can be seen in the comparison of the two displacement fields. The deformation of the control panel can be characterized as a series of flat concrete panels hinged at the

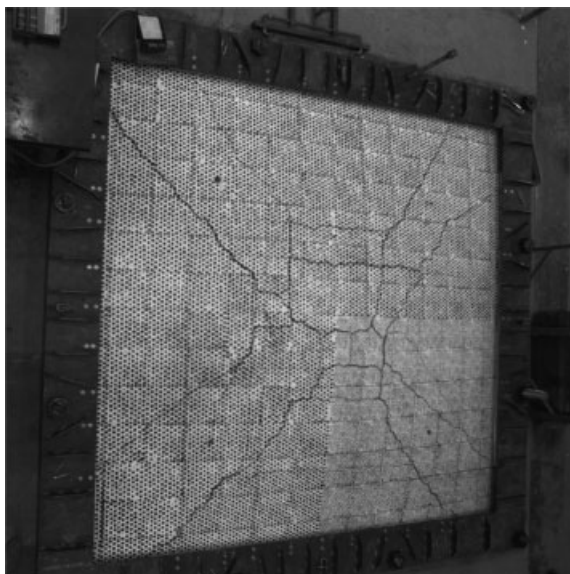


Fig. 6 View from global camera 0 showing cracking at the maximum load in the non-reinforced specimen

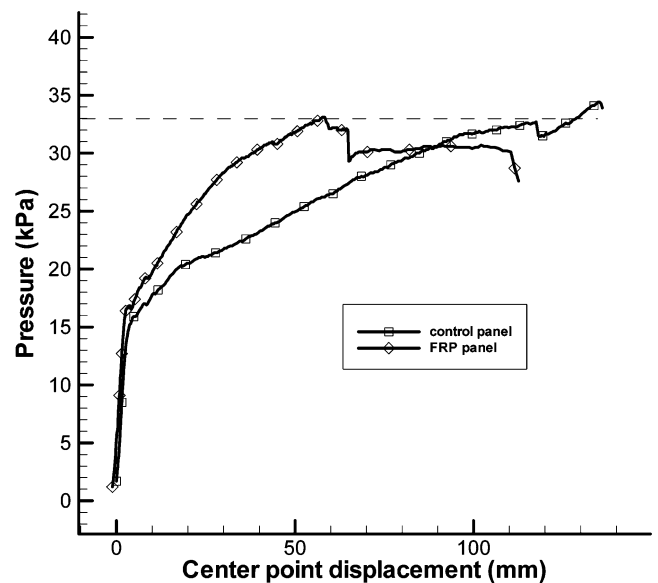


Fig. 7 Comparison of the centre point displacements from the control and FRP-reinforced panels

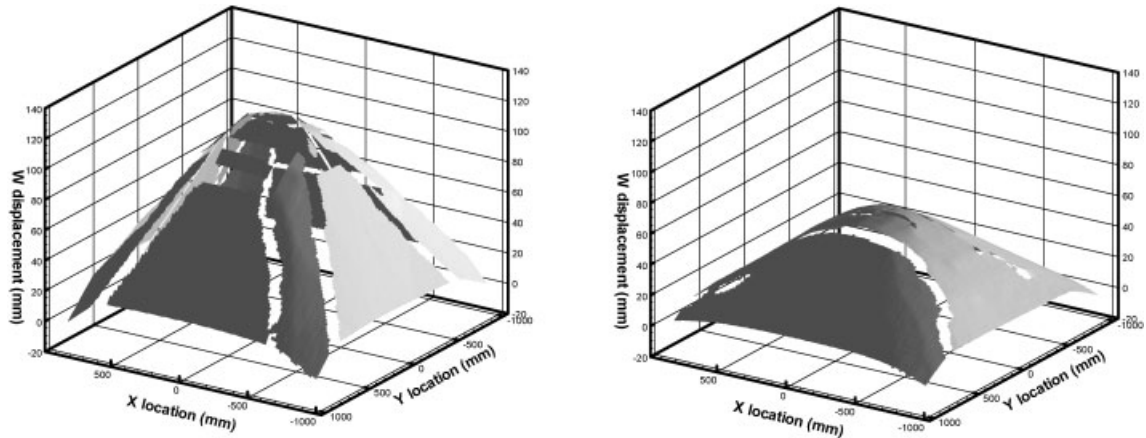


Fig. 8 Out-of-plane displacements of the control and FRP-reinforced panels at maximum load

crack locations. By contrast, the FRP strips helped to maintain the integrity of the tensile surface, thus reducing the faceting of the surface deformation. This results in the lessened and more curvaceous deformation.

The extent of cracking in the two panels is easily seen in the contour plots of the magnitude of the first principal strain shown in Fig. 9. Any cracking behaviour not rejected by the exclusion portion of the DIC program will show up as a peak in the strain plot or as a gap in the contour data. The location of the three FRP strips is shown as a white outline on the contour plot. The strain contours in the global areas are less defined than those in the local strain fields because of the difference in the spatial resolution of the two data sets. As seen in this figure, the FRP strips maintained the integrity of the central portion of the panel and greatly

reduced the degree of surface cracking, particularly in the Y direction.

The effect of the FRP strips on the crack propagation through the panel can be seen in Fig. 10 which superimposes the contours from Fig. 9 on a rendering of the initial shape of the panel. For clarity the lowest strain contour has been omitted to highlight the crack paths. At the maximum load, none of the FRP strips on the specimen had ruptured and the panel failed as crack paths developed between the FRP strips and propagated beyond the ends of the strips. It is apparent from the figure that, while the FRP strips acted to defuse the strain in the panels, the cracks grew through the underlying substrate. This is also visible in the graph of strain values calculated along the centre-line of the FRP strips shown in Fig. 11. At locations where cracks grew under the FRP, spikes in the strain data can be observed.

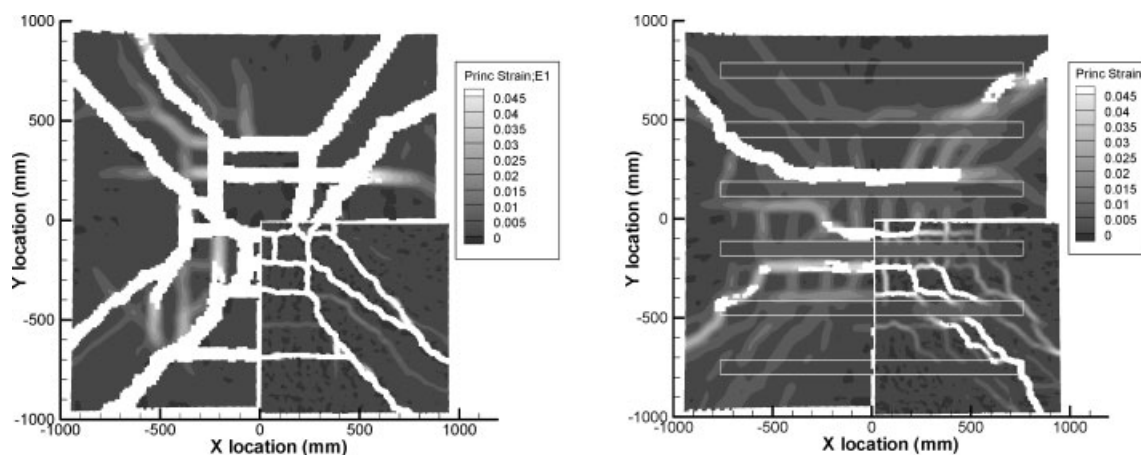


Fig. 9 First principal strains in the control and FRP panels. White rectangles indicate FRP strip locations

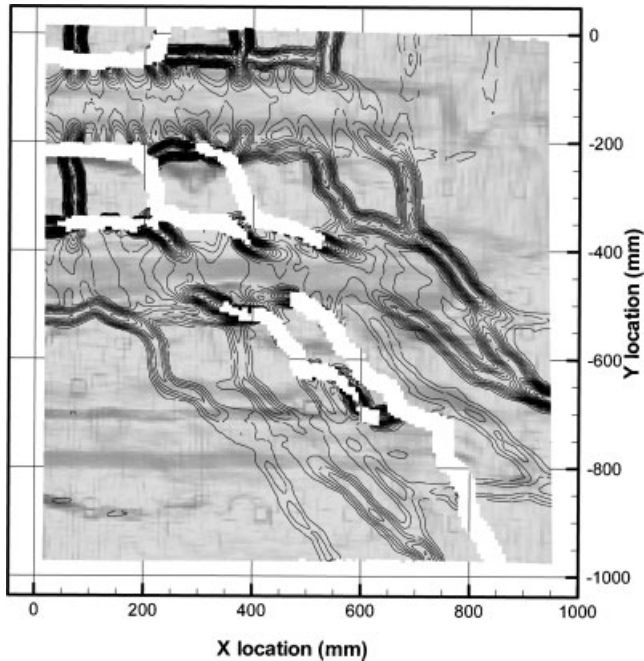


Fig. 10 First principal strain contours superimposed on the initial panel shape from the local camera system

5 CONCLUSIONS

A loading system designed for the study of FRP-reinforced concrete panels has been presented. The system is capable of applying a distributed load to reinforced concrete panels approximately $2\text{ m} \times 2\text{ m}$ in size. Because the system requires no obstructions to the top surface of the specimen, it allowed the use of DIC techniques. The loading frame maintains a hinged boundary condition at the interface with the panels while still allowing horizontal movement of the hinge and without constraining movement of the corners of the panel. Because the load is applied by introducing a volume of water, the tests are run under an effective and safe displacement control.

DIC was used to obtain full-field displacement and strain measurements. Images were taken at two spatial resolutions. The global system was capable of imaging the entire surface in each image; however, analysis was restricted to three quarters of the panel owing to the applied patterns. The local system imaged the remaining quarter of the panel at twice the spatial resolution of the global system. Because of the widespread cracking in the specimen, a crack exclusion method was devised for and incorporated into the DIC process.

Results comparing the cracking and displacement behaviour of an unstrengthened control concrete specimen with that of a specimen with six unidirectional FRP strips were presented.

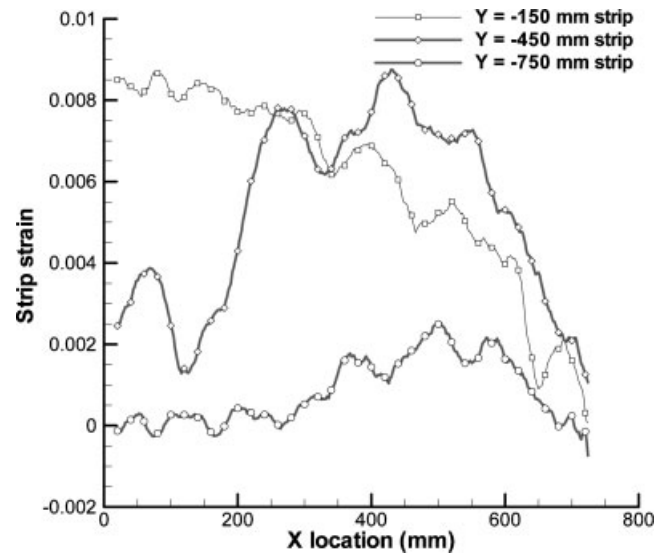


Fig. 11 Longitudinal strain in the FRP strips at maximum load

While the failure load of the FRP panel was not significantly higher than that of the control panel, the amount of out-of-plane displacement was cut roughly in half. It was observed that the deformed shape of the control specimen was formed by a number of relatively flat panels hinged together at crack locations. The strengthened specimen showed less of this faceting as the FRP strips maintained the integrity of the tensile surface to a great degree. Closer inspection of the strain fields from the local camera system showed that, while the FRP strips were successful in distributing the strains in the cracked areas, the effects of the cracks did migrate under the FRP strips.

The work in this paper presents a simple and yet effective loading system to test two-way steel-reinforced concrete slabs. The system can apply a uniform pressure load, operates under displacement control, and imposes known edge conditions on the specimen. The load system, coupled with the full-field capabilities of the DIC method, provides a test system uniquely suited to the study of reinforced concrete panels.

ACKNOWLEDGEMENTS

The research equipment for this work was purchased from the National Science Foundation MRI Grant 0319846. The authors also wish to acknowledge the work of Harry Folk, Keith Moon, and Kevin Farrell of the Lafayette College Machine Shop.

REFERENCES

- 1 Ritchie, P. A., Thomas, D. A., Lu, L.-W., and Connelly, G. M. External reinforcement of concrete beams using fiber reinforced plastics. *ACI Struct. J.*, 1991, **88**(4), 490–499.
- 2 Saadatmanesh, H. and Ehsani, M. R. RC beams strengthened with GFRP plates I: experimental study. *J. Struct. Engng*, 1991, **117**(11), 3417–3433.
- 3 Sharif, A., Al-Sulaimani, G. J., Basunbul, I. A., Baluch, M. H., and Ghaleb, B. N. Strengthening of initially loaded reinforced concrete beams using FRP plates. *ACI Struct. J.*, 1994, **91**(2), 160–168.
- 4 Chajes, M. J., Januszka, T. F., Mertz, D. R., Thomson Jr, T. A., and Finch Jr, W. W. Shear strengthening of reinforced concrete beams using externally applied composite fabrics. *ACI Struct. J.*, 1995, **92**(3), 295–303.
- 5 Arduini, M. and Nanni, A. Behaviour of precracked RC beams strengthened with carbon FRP sheets. *J. Composites Constr.*, 1997, **1**(2), 63–70.
- 6 Kurtz, S. and Balaguru, P. Comparison of inorganic and organic matrices for strengthening of RC beams with carbon sheets. *J. Struct. Engng*, 2001, **127**(1), 35–42.
- 7 Colotti, V., Spadea, G., and Swamy, R. N. Structural model to predict the failure behavior of plated reinforced concrete beams. *J. Composites Constr.*, 2004, **8**(2), 104–122.
- 8 Roberts, T. M. Approximate analysis of shear and normal stress concentrations in the adhesive layer of plated RC beams. *Struct. Engrg*, 1989, **67**(12), 229–233.
- 9 Täljsten, B. Strengthening of beams by plate bonding. *J. Mater. Civil Engng*, 1997, **9**(4), 206–212.
- 10 Malek, A. M., Saadatmanesh, H., and Ehsani, M. R. Prediction of failure load of R/C beams strengthened with FRP plate due to stress concentration at the plate end. *ACI Struct. J.*, 1998, **95**(1), 142–152.
- 11 Rasheed, H. A. and Pervaiz, S. Bond slip analysis of fiber-reinforced polymer-strengthened beams. *J. Engng Mechanics*, 2002, **128**(1), 78–86.
- 12 Mukhopadhyaya, P. and Swamy, N. Interface shear stress: a new design criterion for plate debonding. *J. Composites Constr.*, 2001, **5**(1), 35–43.
- 13 Kurtz, S., Balaguru, P., and Helm, J. Experimental study of interfacial shear stresses in FRP-strengthened RC beams. *J. Composites Constr.*, 2008, **12**(3), 312–322.
- 14 Kurtz, S., Barker, M., and Schlicht, M. Uniform load testing of CFRP-strengthened RC beams. *ACI Struct. J.*, 2008 (submitted).
- 15 Helm, J. Digital image correlation for specimens with multiple growing cracks. *Expl Mechanics*, 2008 DOI.10.1007/s11340-007-9120-2.